Molecular Genetics and Metabolism 143 (2024) 108538

Contents lists available at ScienceDirect

Molecular Genetics and Metabolism

journal homepage: www.elsevier.com/locate/ymgme

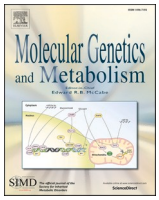

HepG2 PMM2-CDG knockout model: A versatile platform for variant and therapeutic evaluation

Alicia Vilas [a,b,c,1], Álvaro Briso-Montiano [a,b,c,1], Cristina Segovia-Falquina [a,b,c,1], Arturo Martín-Martínez [a,b,c], Alejandro Soriano-Sexto [a,b,c], Diana Gallego [a,b,c], Vera Ruiz-Montés [a,b,c], Alejandra Gámez [a,b,c], Belén Pérez [a,b,c,*]

[a] Centro de Diagnóstico de Enfermedades Moleculares, Centro de Biología Molecular-SO UAM-CSIC, Universidad Autónoma de Madrid, Campus de Cantoblanco, 28049 Madrid, Spain
[b] U746 - CIBER de Enfermedades Raras (CIBERER), Madrid, Spain
[c] Instituto de Investigación Sanitaria IdiPAZ, Madrid, Spain

ARTICLE INFO

Keywords:
Phosphomannomutase 2 deficiency (PMM2-CDG)
HepG2
Disease model
CRISPR-Cas9
Knockout
Variant evaluation
Therapeutic strategies

ABSTRACT

Phosphomannomutase 2 deficiency (PMM2-CDG), the most frequent congenital disorder of glycosylation, is an autosomal recessive disease caused by biallelic pathogenic variants in the *PMM2* gene. There is no cure for this multisystemic syndrome. Some of the therapeutic approaches that are currently in development include mannose-1-phosphate replacement therapy, drug repurposing, and the use of small chemical molecules to correct folding defects. Preclinical models are needed to evaluate the efficacy of treatments to overcome the high lethality of the available animal model. In addition, the number of variants with unknown significance is increasing in clinical settings. This study presents the generation of a cellular disease model by knocking out the *PMM2* gene in the hepatoma HepG2 cell line using CRISPR-Cas9 gene editing. The HepG2 knockout model accurately replicates the PMM2-CDG phenotype, exhibiting a complete absence of PMM2 protein and mRNA, a 90% decrease in PMM enzymatic activity, and altered ICAM-1, LAMP1 and A1AT glycoprotein patterns. The evaluation of *PMM2* disease-causing variants validates the model's utility for studying new *PMM2* clinical variants, providing insights for diagnosis and potentially for evaluating therapies. A CRISPR-Cas9-generated HepG2 knockout model accurately recapitulates the PMM2-CDG phenotype, providing a valuable tool for assessing disease-causing variants and advancing therapeutic strategies.

1. Introduction

Phosphomannomutase 2 deficiency or PMM2-CDG (MIM# 212065) is the most common congenital disorder of glycosylation (CDG) with an estimated prevalence of 1:20,000 in some populations [1,2]. It is an autosomal recessive disorder caused by pathogenic variants in the *PMM2* gene (MIM# 601785). *PMM2* is located on chromosome 16p13 and encodes the phosphomannomutase 2 (PMM2) enzyme (EC_5.4.2.8) [3]. This homodimeric enzyme catalyzes the reversible conversion of mannose-6-phosphate (M6P) to mannose-1-phosphate (M1P) in the cytosol [4,5], the second step in the synthesis of guanosine-diphosphate-mannose (GDP-Man). GDP-Man is a critical component in glycoconjugate synthesis; thus, the alteration of this reaction affects the entire N-glycosylation pathway [6] and causes metabolic dysfunction [7–10].

PMM2 deficiency is considered a multisystemic disease [11,12]. Patients with PMM2-CDG exhibit highly variable phenotypes with different degrees of severity, ranging from asymptomatic [13] and mild cases with slight neurological impairment [14] to highly severe cases that can cause death in the first days of life [15]. The most severe clinical presentation consists of both neurological and extra-neurological manifestations, including growth failure, hypotonia, dysmorphic features, liver, kidney, gastrointestinal, and cardiac problems, coagulopathies, recurrent infections, edema, and hormonal imbalances [11,16]. Approximately 20–25% of patients die before the age of five, often due to multiorgan failure or immunological issues [17–19].

Despite being the first described CDG [20], this disease still has no

* Corresponding author at: Centro de Diagnóstico de Enfermedades Moleculares, Centro de Biología Molecular-SO UAM-CSIC, Universidad Autónoma de Madrid, Campus de Cantoblanco, 28049 Madrid, Spain.
E-mail addresses: bperez@cbm.csic.es, belen.perez@uam.es (B. Pérez).
[1] Joint first authors

https://doi.org/10.1016/j.ymgme.2024.108538
Received 19 February 2024; Received in revised form 28 June 2024; Accepted 15 July 2024
Available online 17 July 2024

cure. The most promising therapeutic approaches proposed so far involve therapies designed to increase the availability of M1P and/or GDP-Man [21], (https://www.glycomine.com/), drug repurposing based on the pathophysiology [22,23], and those focused on enhancing the concentration and/or activity of hypomorphic PMM2 mutants [24,25]. Some of these approaches have already reached the clinical trial phase: GLM101 M1P replacement therapy from Glycomine (ClinicalTrials.gov identifier: NCT05549219) and the repurposed drugs epalrestat (ClinicalTrials.gov identifier: NCT04925960) and acetazolamide (ClinicalTrials.gov identifier: NCT04679389).

In the genomic era, early diagnosis of PMM2-CDG remains challenging, despite carrier and neonatal screening, and symptomatic diagnosis [26–29], the growing number of variants of unknown significance (VUS) further complicates the diagnosis process [30]. Current high-throughput systems, such as our recently developed prokaryotic system, are not well-suited for evaluating the effect of *PMM2* variants in a physiological environment, thus limiting their clinical utility [31].

Disease models play a crucial role in drug discovery and development [32,33]. The scope of PMM2-CDG models encompasses not only patient-derived fibroblasts but also prokaryotic systems for expressing recombinant proteins, three-dimensional structures, and various cellular and animal models [10,22,34–45]. Although fully replicating the complex and variable phenotype of PMM2-CDG represents a challenge, each model has significantly contributed to advancing research in this disease. For instance, the *C. elegans* model facilitated the identification of a potential treatment for PMM2-CDG through drug repurposing [22]. Zebrafish models have provided insights into embryonic development, neurogenesis, endoplasmic reticulum stress and other altered pathways in PMM2 deficiency [42,43,45]. The generation of mouse models is still challenging due to the high embryonic lethality associated with some genotypes [40] and to the fact that not all the clinical features observed in human patients are present in the available mouse models, particularly the neurological symptoms [44].

Patient-derived fibroblasts are widely employed models for diagnosing and researching many rare diseases, such as inborn errors of metabolism, as they allow maintaining the patients' genetic background. Nevertheless, not all genes or markers of pathology are expressed in this cell type [46], and fibroblasts are metabolically inactive cells with a limited lifespan [47,48]. An alternative to using patients´ fibroblasts is the immortalization of primary cultures or the use of established cultures derived from different types of tumours such as hepatoma, neuroblastoma, or cervical cancer [49–53]. Another advantage of cellular models is that they can be easily genetically manipulated with CRISPR-Cas technology to study the pathogenic mechanism of specific variants or the effect of depleting or inserting a particular gene [54,55].

Rare diseases´ research is full of challenges and limitations such as the scarcity of patients´ samples and the development of models to study the pathogenicity, methods for an accurate and rapid diagnosis, and effective treatments. The availability of disease models is essential to identify therapeutic targets and biomarkers, serving as a screening and drug evaluation platform. This project's main objective has been improving the diagnosis and developing therapeutic strategies for PMM2-CDG by generating a cellular PMM2-CDG model. Due to the hepatic involvement described in many PMM2-CDG patients and the exciting possibility of using the liver as a target organ in the drug evaluation process for PMM2 deficiency, this study has focused on the development of a cellular disease model in the hepatoma HepG2 cell line.

A PMM2 knockout (KO) model has been generated that can be used as a platform for functional variant analysis and pharmacological evaluation.

2. Materials and methods

2.1. Cell culture

The hepatoma cell line HepG2 was obtained from ATCC (HB-8085). HepG2, HepG2-KO, and HEK293T cells were cultured under standard conditions in minimal essential medium (MEM) supplemented with 5 or 10% fetal bovine serum (FBS), 1% glutamine and antibiotics (penicillin and streptomycin mix) with a relative humidity of 95%, 5% CO_2, and a temperature of 37 °C.

2.2. Karyotyping

Cells were treated with 10 μg/ml Colcemid® Solution (Irvine Scientific, USA) for 90 min at 37 °C, harvested with trypsin, treated with hypotonic solution, and fixed with Carnoy's fixative for karyotype analysis at *Centro Nacional de Investigaciones Oncológicas* (CNIO, Madrid, Spain). The minimum number of analyzed metaphases was 20.

2.3. Generation of the PMM2 knockout model

The bioinformatics tool Breaking-Cas (https://bioinfogp.cnb.csic.es/tools/breakingcas/) was used for the design of RNA guides (gRNA) that targeted exon 5 of the *PMM2* gene. Only the two gRNA with the higher score and lower probabilities of producing off-targets were selected (gRNA1: ATGTTAAACGTGTCCCCTAT; gRNA2: CTTTCATTGAATTCCGAAAT).

The Alt-R CRISPR-Cas9 System and *Streptococcus pyogenes* Cas9 (SpCas9) nuclease (Integrated DNA Technologies, IDT, USA) were used following the supplier's recommendations for knockout generation. After reverse transfection of 800,000 HepG2 cells per well of a 6-well plate with the ribonucleoproteins (RNP), the transfection efficiency was checked by measuring the fluorescent signal from the Alt-R CRISPR-Cas9 tracrRNA ATTOTM 550 (IDT). For the cell sorting, cells were harvested with trypsin and collected in sorting buffer (PBS, 5 mM EDT, 2% FBS, HEPES pH 7) at a cell density of <15 million cells/ml. Positive cells were seeded again into 150 mm cell culture dishes to form single-cell colonies. Colonies were isolated by manually picking and seeding into individual wells of 24-well plates. The candidate cell populations were then expanded into 12-well and 6-well plates.

2.4. PCR mismatch

Genomic DNA was extracted from the candidate cell populations with the QIAmp DNA Mini kit (QIAGEN, Germany) following the manufacturer's recommendations. Editing was verified by PCR Mismatch using 100 ng of DNA from each population, specific primers (Suppl. Table 1), and the Supreme NZYTaq II 2× Green Master Mix (NZYTech, Lisbon).

2.5. Sanger sequencing and targeted deep sequencing

Approximately 250–500 ng of genomic DNA were sequenced by the company Macrogen® using specific oligonucleotides at 5 μM (Suppl. Table 1) and the enzymatic chain-termination DNA sequencing method described by Sanger et al., 1977 [56]. Samples for targeted deep sequencing were prepared following the instructions of the *Parque Científico de Madrid* and, next, sequenced on a MiSeq sequencer (Illumina, USA). The bioinformatics analysis of the targeted deep sequencing was carried out at the *Centro de Diagnóstico de Enfermedades Moleculares* (CEDEM, Madrid, Spain).

2.6. Quantitative RT-PCR

The three predicted off-targets for gRNA1 with the highest score as provided by the Breaking-Cas software and *PMM2* mRNA levels were checked by RT-qPCR as described elsewhere [25] with specific oligonucleotides (Suppl. Table 1).

2.7. Western blot analysis

Cells were harvested with scraper and resuspended in RIPA buffer (50 mM Tris-HCl pH 7.4, 150 mM NaCl, 1% Triton X-100, 0.5% sodium deoxycholate, 0.1% SDS) containing Complete Mini EDTA-free Protease Inhibitor Cocktail (Roche, Switzerland). Lysis was achieved by pipetting the cell suspension and freezing at −80 °C for at least 30 min. Next, samples were thawed and lysed with a 22-gauge needle and, finally, centrifuged for 10 min at maximum speed and 4 °C to collect the supernatant. Protein concentration was quantified using the Bradford assay (BioRad, USA). The samples for the electrophoretic separation were prepared in NuPage®LDS 4× sample buffer (Invitrogen, USA) and dithiothreitol (DTT); after that, they were heated at 70 °C for 10 min. The electrophoresis was performed in 4–12% NuPAGE Novex Bis-Tris mini gels (Invitrogen), or in 12% acrylamide/bisacrylamide handmade gels. The selected molecular weight marker was the ProSieve Color Protein Marker (Lonza, Switzerland). Following the electrophoretic separation, proteins were transferred to a nitrocellulose membrane using the iBlot Gel Transfer Stacks Nitrocellulose Regular (Invitrogen) in an iBlot2 Transfer System (Invitrogen). Membranes were blocked for at least 1 h with TBS 0.05% Tween and 5% low-fat milk at room temperature. Immunodetections were performed using PMM2 antibody at 1:1000 (10666–1-AP, Proteintech, USA), ICAM-1 antibody at 1:1000 (sc-7891; Santa Cruz Biotechnology, USA), LAMP1 antibody at 1:1000 (3243, Cell signaling, USA), A1AT antibody at 1:500 (sc-59438; Santa Cruz), GAPDH antibody at 1:5000 (ab8245, Abcam, UK) and β-actin antibody at 1:5000 (TA811000S; Origene, USA). The secondary antibodies used were goat anti-rabbit IgG horseradish peroxidase-linked antibody at 1:5000 (7074S, Cell Signaling, USA) and horse anti-mouse IgG horseradish peroxidase-linked antibody at 1:2000 (7076S, Cell Signaling). Two detection methods were used depending on the intensity of the signal: SuperSignal West Femto Maximum Sensitivity Substrate (ThermoFisher, USA) for low signal substrates and Enhanced Chemiluminescence System (GE Healthcare, UK) for high signal substrates.

2.8. PNGaseF treatment

HepG2 and HepG2-KO cells were lysed in lysis buffer (10 mM Tris, 150 mM NaCl, 10% glycerol, 0.1% Triton X-100) with Complete Mini EDTA-free Protease Inhibitor Cocktail (Roche). Next, cell suspensions were frozen in liquid nitrogen for 5 min, followed by a 5 min-incubation at 37 °C. This process was repeated three times before centrifuging the samples for 10 min at maximum speed and 4 °C for collecting the supernatant. The protein content in the samples was quantified with the Bradford method, and the corresponding volume of cell extract was denaturalized and digested with PNGaseF (New England Biolabs, USA) following the manufacturer's recommendation. The digestion was analyzed by western blotting as previously specified.

2.9. Lentiviral transduction

The HepG2-KO model was used to introduce different *PMM2* clinical variants (c.53C > G (p.Thr18Ser), c.131 T > C (p.Val44Ala), c.193G > T (p.Asp65Tyr), c.194 > G (p.Asp65Gly), c.338C > T (p.Pro113Leu), c.357C > A (p.Phe119Leu), c.367C > T (p.Arg123*), c.484C > T (p.Arg162Trp), c.710C > T (p.Thr237Met) and c.710C > A (p.Thr237Lys)) by lentiviral transduction. Two different lentiviral constructions were generated, one with the pReceiver-Lv101 plasmid (GeneCopoeia, USA), containing the *PMM2* cDNA coupled to a FLAG tag (LV-FLAG system), and another with the pReceiver-Lv103 plasmid (GeneCopoeia) with the *PMM2* cDNA fused to the coding sequence of the green fluorescent protein (GFP) (LV-GFP system). The variants were introduced in the plasmids with the QuikChange Site-Directed Mutagenesis kit (Agilent, USA) following the manufacturer's instructions and using specific oligonucleotides (Suppl. Table 1).

2.10. Phosphomannomutase enzymatic activity assay

Phosphomannomutase (PMM) enzymatic activity was measured in the cellular extract of the HepG2 cells, HepG2-KO cells, and in the HepG2-KO cells transduced with the different lentiviral particles. To that end, 20,000 cells per well for the LV-FLAG lines and 10,000 cells per well for the LV-GFP lines were seeded in 96-well plates and incubated for 72 h at 37 °C. The assay was performed using the method of Van Schaftingen and Jaeken [57] after the modifications made by de Koning [58]. The NADPH signal was amplified to improve the detection method using the Amplite® Fluorimetric NADP/NADPH Ratio Assay Kit Red Fluorescence (AAT Bioquest, USA) [35].

The production of the lentiviral particles and the infection of the HepG2-KO cells were performed as described elsewhere [59]. Efficiently infected HepG2-KO cells were selected by geneticin treatment at 2 mg/ml (Lv-101 vector) or by puromycin treatment at 2.5 μg/ml (Lv-103 vector), depending on the system. The antibiotic concentrations were reduced to 1 mg/ml and 1 μg/ml, respectively, for maintaining the cell lines after selection.

2.11. Proliferation assay

Following the manufacturer's instructions, cell proliferation was evaluated through the CCK8 assay (Abcam). HepG2 cells were seeded into a 96-well plate at 10,000 cells per well and grown overnight. CCK8 reagent was added to the culture medium at 0, 24, 48, 72 and 96 h after seeding to reach a final concentration of 10%. After 1 h of incubation at 37 °C, absorbance at 460 nm was measured to assess the generation of the formazan product by viable cells.

2.12. Trypan blue staining

A total of 135,000 HepG2 cells were seeded into a 35 mm plate and grown overnight. Cells were stained with 0.4% trypan blue (Sigma-Aldrich, USA) at 0, 24, 48, 72 and 96 h and alive cells were counted in a hemocytometer.

2.13. Statistical analysis

The statistical analysis was performed using GraphPad Prism 8.0.2 (GraphPad Software Inc.). Data were expressed as mean ± SD. Statistical significance was determined using the Student's *t*-test to compare two groups and Ordinary One-way ANOVA or Two-way ANOVA with Dunnet's correction for multiple comparisons. A *p*-value of <0.05 was considered statistically significant (* $p < 0.05$, ** $p < 0.01$, *** $p < 0.001$).

3. Results

3.1. The HepG2 PMM2 knockout model recapitulates the PMM2-CDG cellular phenotype

The PMM2-CDG KO model was generated through the CRISPR-Cas9 gene editing system of the human hepatoma cell line HepG2. Before the genetic editing, karyotype analysis of HepG2 cells confirmed that there were no numerical or large structural anomalies affecting chromosome 16, in which the *PMM2* gene is located (**Suppl Fig. 1**). To obtain the model, HepG2 cells were transfected with two different RNA guides targeting exon 5. This exon encodes amino acids between positions 117 to 149, including some residues that are highly conserved and crucial for the dimerization and the enzymatic activity of PMM2, such as Phe119, Arg123, Arg134 and Arg141 [31,34,35,37] (Fig. 1A). The analysis of the candidate cell populations by PCR mismatch showed that 15 colonies had been edited (data not shown). PMM2 protein levels were checked in these 15 candidate populations, and there were undetectable levels of PMM2 protein in 8 populations, all edited with guide 1 (Fig. 1B).

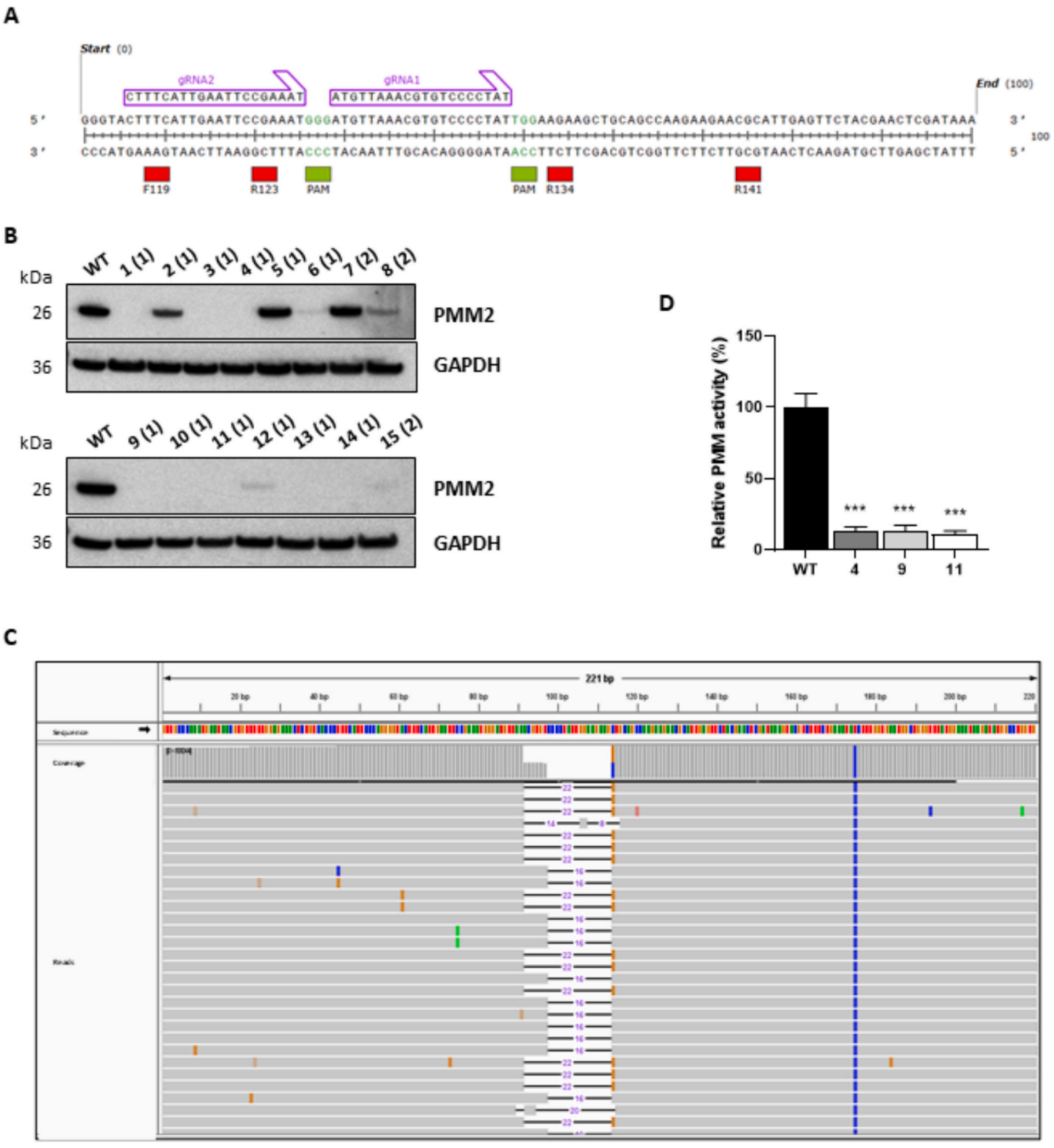

Fig. 1. Generation of the PMM2-CDG knockout model in HepG2 cells. (**A**) Nucleotide sequence of *PMM2* exon 5 and sequences of the two guide RNA specifically designed for the knockout of *PMM2*, gRNA1 and gRNA2. The PAM sequences are highlighted in green, and the codons that codify crucial aminoacids for PMM2 function (F119, R123, R134 and R141) are indicated in red. (**B**) Immunodetection of PMM2 in the selected cell populations, from 1 to 15. The number between brackets indicate the gRNA used for their edition, gRNA1 (1) or gRNA2 (2). Same amounts of total protein from the soluble extracts were loaded onto SDS-PAGE gels. GAPDH was used as loading control. (**C**) Targeted deep sequencing reads of cell population 4 in the Integrative Genomics Viewer (IGV) showing the nucleotide sequence of *PMM2* exon 5, the coverage, and the reads with the 16-bp and 22-bp deletions. (**D**) Relative PMM enzymatic activity of cell populations 4, 9 and 11 expressed as a percentage (%) considering that the enzymatic activity of HepG2 wildtype cells (WT) is the 100%. Data represents the mean ± SD of at least three independent experiments (*** $p < 0.001$). (For interpretation of the references to color in this figure legend, the reader is referred to the web version of this article.)

After Sanger sequencing analysis of exon 5 of *PMM2*, only candidate cell populations 4, 9, and 11 revealed insertions and/or deletions in both alleles (data not shown). To confirm the complete absence of wildtype (WT) sequences in the three most promising candidates, an analysis of mosaicism by targeted deep sequencing was performed. The cell populations 9 and 11 showed WT reads undetected by Sanger sequencing. On the contrary, cell population 4, exhibited no WT sequences and showed a deletion of 16 base pairs (bp) and 22 bp in different alleles (Table 1) (Fig. 1C). The potential off-targets predicted for guide 1 were checked in the candidate populations, and no modifications were observed in these regions after the editing (data not shown).

The phosphomannomutase (PMM) enzymatic activity was measured in cell populations 4, 9, and 11. A substantial reduction in PMM activity compared to WT cell line was observed in the three populations (Fig. 1D). Given all the results, cell population 4 was considered a clone (HepG2-KO clone) and was selected for further studies.

The PMM2 expression levels were analyzed in the HepG2-KO, showing no *PMM2* mRNA in the KO in comparison with the *PMM2* mRNA levels in the HepG2 cells (Fig. 2A). The HepG2-KO clone was further characterized by studying the effect of PMM2 absence in three glycoproteins: intercellular adhesion molecule 1 (ICAM-1), lysosomal associated membrane protein 1 (LAMP1), and alpha-1-antitrypsin (A1AT). ICAM-1 is a membrane protein with 8 glycosylation sites, LAMP1 is a lysosomal membrane protein with 18 glycosylation sites, and A1AT is a plasma serine protease inhibitor (serpin) with 6 glycosylation sites (https://glyconnect.expasy.org/). The western blot revealed that in the HepG2-KO line, the three proteins presented an altered band pattern, showing changes in their electrophoretic mobility (Fig. 2B). Next, cell extracts were treated with peptide-N-glycosidase F or PNGaseF, an amidase that removes N-linked oligosaccharides by cleaving between the *N*-acetylglucosamine (GlcNAc) and the asparagine residues. The aim was comparing the pattern of the glycoproteins in the HepG2 WT and the HepG2-KO after completely removing the N-glycans. Interestingly, the molecular weight of the non-glycosylated bands of ICAM-1, LAMP1, and A1AT was lower than the molecular weight of the bands of both glycoproteins in the untreated KO sample (Fig. 2C).

The HepG2-KO model was transduced with a lentiviral vector carrying the *PMM2* WT cDNA (LV-WT) or an empty vector to confirm that the phenotype observed in the genetically modified cells was only due to the deletion of the *PMM2* gene if it can be reversed by restoring the PMM2 function. In this experiment, the GFP lentiviral system was used. PMM2 protein levels were restored after transduction with the LV-WT. The altered glycosylation pattern of the LAMP1 and ICAM-1 proteins was also corrected in the LV-WT transduced cells. Neither PMM2 protein levels nor the glycosylation pattern of LAMP1 and ICAM-1 were recovered when the KO cells were transduced with the empty vector (Fig. 2D). The enzymatic activity assay showed a significant increment in the PMM activity measured in the KO line recovered with the LV-WT compared to the activity measured in the HepG2 WT cells and the KO cells (Fig. 2E).

Proliferation was analyzed in the HepG2 WT, in the HepG2-KO cells and in the KO recovered with the LV-WT to check if the PMM2-CDG model had cell growth affected. The results from the CCK8 assay didn't show significant differences in the proliferation of any of the three cell lines at 24 and 48 h, however, at 72 h, there was a decrease in the WT cell line proliferation (Fig. 2F). These results were confirmed by cell counting of viable cells with Trypan Blue staining. Similar numbers of cells were registered for the three cell lines at 24, 48 and 72 h (Fig. 2G).

3.2. *PMM2-CDG knockout model is successfully used for pathogenic validation of clinical variants*

Once the PMM2 KO model was characterized, it was used to express and study the effect of several *PMM2* clinical variants by stable expression. Two different lentiviral systems were initially tested, one with the cDNA of *PMM2* fused to GFP (LV-GFP) and the other fused to the FLAG epitope (LV-FLAG).

First, we expressed five previously characterized destabilizing hypomorphic mutants (p.Val44Ala, p.Asp65Tyr, p.Pro113Leu, p.Arg162Trp, and p.Thr237Met) and one variant affecting the dimerization of the protein (p.Phe119Leu) [31,35]. After introducing in the HepG2-KO cells the corresponding variants, we studied their effect on PMM activity and their functionality by analysis of the glycosylated proteins LAMP1, ICAM-1 and A1AT.

The enzymatic activity ranged from 6.4 ± 2.5% to 42.5 ± 29.6% with the LV-GFP system and from 8.3 ± 5.3% to 21.6 ± 5.6% with the LV-FLAG system. Four mutant proteins (p.Val44Ala, p.Asp65Tyr, p.Pro113Leu, and p.Phe119Leu) exhibited an activity lower than 20% of the activity detected in the LV-WT in both systems. The activity of p.Arg162Trp and p.Thr237Met was higher than 20%, independently of the LV expression system. The PMM enzymatic activity was slightly higher when PMM2 was expressed fused to GFP than the activity of the mutants with the FLAG tag for three of the studied mutants: p.Pro113Leu, p.Arg162Trp, and p.Thr237Met (Fig. 3A). Since the fusion of the GFP protein to the mutant PMM2 proteins could be interfering in their residual activity, the following experiments were performed only with the LV-FLAG system. Regarding the glycosylation of ICAM-1, LAMP1 and A1AT, no qualitative differences were observed in the band pattern of ICAM-1 among the different cell lines, while LAMP1 glycosylation showed an alteration in the p.Pro113Leu, p.Arg162Trp, and the p.Thr237Met cell lines. The band of A1AT observed in all the variant cell lines was similar to the high molecular weight band of A1AT in the WT cells, although for this glycoprotein, the LV-WT recovery was not as clear as it was with ICAM1 or LAMP-1. The nonsense mutant p.Arg123* showed a change in the electrophoretic mobility of ICAM-1, LAMP1 and A1AT, although the band pattern of A1AT showed an intermediate electrophoretic mobility between the one observed in the WT cells and in the KO cells (Fig. 3B).

This model was also used to evaluate the effect of three VUS: p.Asp65Gly, p.Thr237Lys and p.Thr18Ser. The two first variants, p.Asp65Gly, and p.Thr237Lys, could not be expressed in the reported

Table 1
Targeted deep sequencing of *PMM2* exon 5 in candidate cell populations.

	STRAND	WT	ins_1bp	del_1bb	del_8bp	del_9bp	del_4bp	del_16bp	del_22bp	TOTAL READS
	+	0					1	20,649	24,207	44,857
4	−	0					0	20,624	24,850	45,474
	TOTAL	0					1	41,273	49,057	90,331
	+	2	1		16,138	7364	7104	1		30,610
9	−	1	0		15,361	7133	7151	0		29,646
	TOTAL	3	1		31,499	14,497	14,255	1		60,256
	+	10	17,503	19,784	2					37,299
11	−	5	16,202	19,303	1					35,511
	TOTAL	15	33,705	39,087	3					72,810
	+	49,924					1			49,925
WT[1]	−	48,015					0			48,015
	TOTAL	97,939					1			97,940

WT[1]: HepG2 wildtype cells. Abbreviations: WT: wildtype; ins: insertion; bp: base pairs; del: deletion.

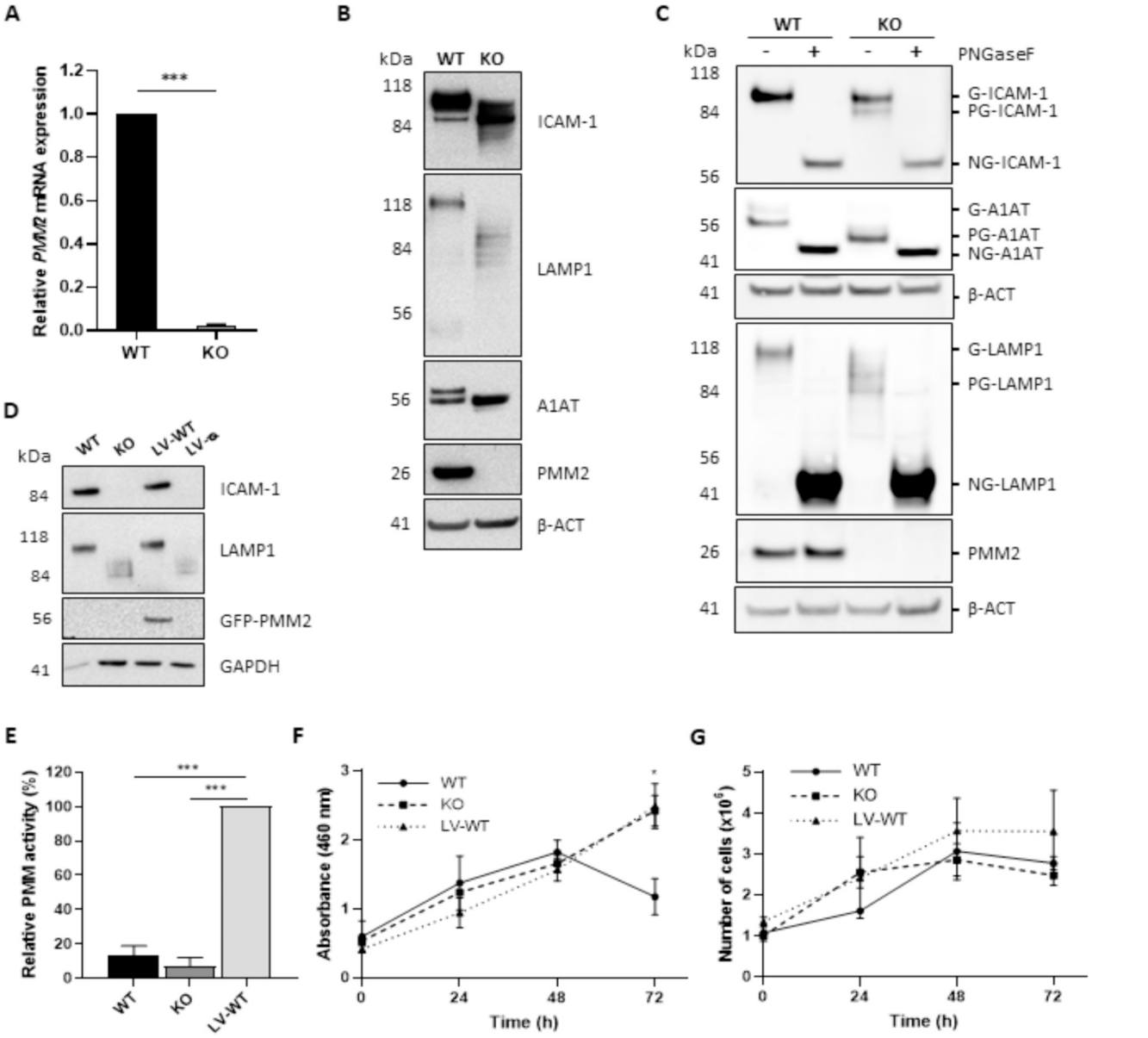

Fig. 2. Characterization of the HepG2 PMM2 KO. (**A**) *PMM2* mRNA expression levels in the knockout model (KO) relative to the *PMM2* mRNA levels in the HepG2 wildtype cells (WT), considered 1′. (**B**) Representative western blot of ICAM-1, LAMP1, A1AT and PMM2. β-actin (β-ACT) was used as loading control. (**C**) Representative western blot of the PNGaseF treatment of the cell extract of treated (+) and untreated (−) HepG2 wildtype (WT) and HepG2-KO (KO) cells. β-actin (β-ACT) was used as loading control. G: glycosylated; PG: partially glycosylated; NG: non-glycosylated; ICAM-1: intercellular adhesion molecule 1; LAMP1: lysosomal associated membrane protein 1; A1AT: alpha-1 antitrypsin. (**D**) Representative western blot of ICAM-1, LAMP1 and PMM2 in HepG2 WT, KO, in the HepG2-KO cells transduced with the lentiviral vector carrying the *PMM2* wildtype cDNA fused with GFP (LV-WT) and in the HepG2-KO cells transduced with the empty GFP lentiviral vector (LV-∅). GAPDH was used as loading control. Same amounts of total protein from the soluble extracts were loaded onto SDS-PAGE gels. (**E**) Relative PMM activity measured in the cellular extract of HepG2 WT, KO and LV-WT, and expressed as percentage (%) considering that the activity of the LV-WT is 100%. Data represents the mean ± SD of at least three independent experiments (*** $p < 0.001$). (**F**) Proliferation of HepG2 WT (solid line, circles), KO (dashed line, squares) and LV-WT (dotted line, triangles) cells measured at 0, 24, 48 and 72 h with the CCK8 assay and expressed as absorbance at 460 nm. Data represents the mean ± SD of at least three independent experiments (* $p < 0.05$). (**G**) Number of viable HepG2 WT (solid line, circles), KO (dashed line, squares) and LV-WT (dotted line, triangles) cells at 0, 24, 48 and 72 h in culture. Data represents the mean ± SD of three technical replicates in one experiment.

prokaryotic system, while p.Thr18Ser presented a high enzymatic activity that initially discarded its pathogenicity [31].

The results confirmed the severe effect on the stability and enzymatic activity of the p.Asp65Gly and the p.Thr237Lys variants. Western blot analysis revealed a total absence of the p.Thr237Lys mutant protein and deficient levels of the p.Asp65Gly mutant (Fig. 4A) with almost null residual activity (<5%) in both cases, comparable to the activity measured in the stop mutant p.Arg123* (Fig. 4B). Concerning the p.Thr18Ser variant, the results showed a similar amount of PMM2 protein compared to the LV-WT cells and a residual PMM activity close to 60% of the activity measured in the LV-WT cell extract (Fig. 4A and B). The analysis of the band pattern of the glycoproteins ICAM-1, LAMP1 and A1AT showed that only the LV-T237K cells reproduced an altered LAMP1 pattern similar to the LAMP1 pattern of the KO and the LV-R123* cells. ICAM1 was neither qualitatively nor quantitatively altered in none of the three evaluated mutants, while A1AT showed a slight molecular weight increase in the cell lines carrying the p.Asp65Gly and the p.Thr237Lys variants (Fig. 4A).

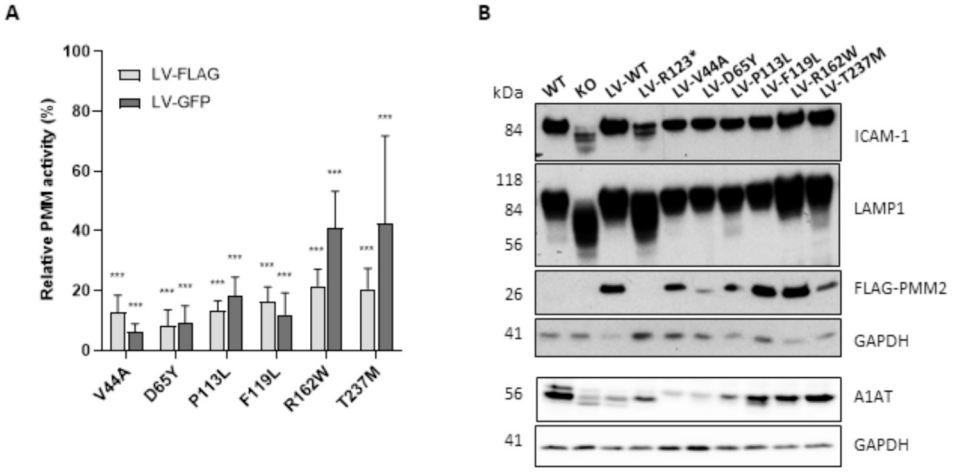

Fig. 3. Characterization of clinical variants in the PMM2-CDG knockout model. (**A**) Relative PMM activity measured in the cellular extract of HepG2-KO cells transduced with the lentiviral vector carrying the *PMM2* cDNA with different clinical variants fused with FLAG (LV-FLAG, clear grey) or GFP (LV-GFP, dark grey), and expressed as percentage (%) considering that the activity of the HepG2-KO cells transduced with the lentiviral vector carrying the *PMM2* wildtype cDNA is 100%. Data represents the mean ± SD of at least three independent experiments (*** $p < 0.001$). (**B**) Representative western blot of ICAM-1, LAMP1, PMM2 and A1AT in the soluble extract of HepG2 WT, KO, KO cells transduced with the FLAG lentiviral vector carrying the *PMM2* wildtype cDNA (LV-WT), HepG2-KO cells transduced with the lentiviral vector carrying the nonsense variant p.Arg123* (LV-R123*) and in the HepG2-KO cells transduced with the FLAG lentiviral vector carrying different PMM2 clinical variants (LV-V44 A, LV-D65Y, LV-P113L, LV-F119L, LV-R162W, LV-T237M). GAPDH was used as loading control. Same amounts of total protein from the soluble extracts were loaded onto SDS-PAGE gels.

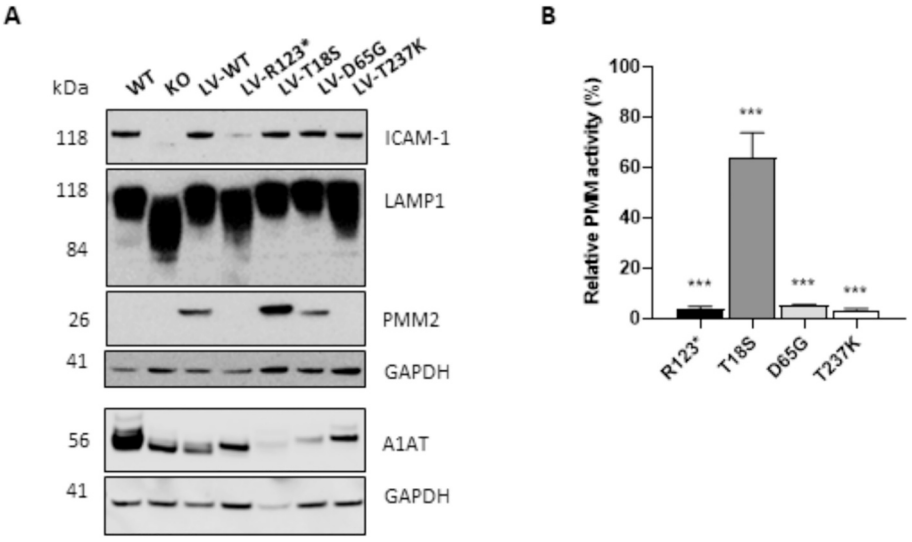

Fig. 4. Characterization of variants of uncertain significance (VUS) in the PMM2-CDG knockout model. (**A**) Representative western blot of ICAM-1, LAMP1, PMM2 and A1AT in the soluble extract of HepG2 wildtype (WT), HepG2-KO (KO), HepG2-KO cells transduced with the lentiviral vector carrying the *PMM2* wildtype cDNA fused with FLAG (LV-WT), HepG2-KO cells transduced with the FLAG lentiviral vector carrying the nonsense variant p.Arg123* (LV-R123*) and in the HepG2-KO cells transduced with the FLAG lentiviral vector carrying different PMM2 VUS (p.Thr18Ser: LV-T18S; p.Asp65Gly: LV-D65G; p.Thr237Lys: LV-T237K). GAPDH was used as loading control. Same amounts of total protein from the soluble extracts were loaded onto SDS-PAGE gels. (**B**) Relative PMM activity measured in the cellular extract of HepG2-KO cells transduced with the FLAG lentiviral vector LV-R123* and in the soluble extract of HepG2-KO cells transduced different VUS (LV-T18S, LV-D65G, LV-T237K). The PMM activity is expressed as percentage (%) considering that the activity of the HepG2-KO cells with the lentiviral vector carrying the *PMM2* wildtype cDNA is the 100%. Data represents the mean ± SD of at least three independent experiments (*** $p < 0.001$).

4. Discussion

The PMM2-CDG HepG2 knockout model presented in this work is the first eukaryotic PMM2 knockout cellular model. This model could be used for pathophysiological studies, assessment of clinical variants, and evaluation of therapeutic strategies such as compounds aimed to increase or decrease the stability or degradation of PMM2 respectively [24,25], or even to evaluate the effect of therapies focused on the recovery of the defective protein [60]. In addition, we have demonstrated its utility for analyzing missense variants identified in the clinical setting.

We have recently described an *in vitro* recombinant protein expression system, which, combined with structural information from the PMM2 crystallographic models [37], demonstrated the pathogenic effect of 15 mutant proteins identified in patients and in a carrier detection program [31]. However, bacterial systems exhibit apparent weaknesses, such as the inability to evaluate the effect of splicing variants, the lack of post-translational protein modifications, and substantial differences in the proteostasis network. Thus, we were unable to confirm the impact of three mutant proteins, p.Asp65Gly, and p.Thr237Lys, which could not

be produced in bacteria, and p.Thr18Ser because its residual enzymatic activity was too high to be considered pathogenic [31]. To bypass these limitations, we generated a PMM2 KO model in HepG2 cells using CRISPR-Cas9 technology and recovered it with WT *PMM2* cDNA or clinical variants.

In this study we also considered other hepatic cell lines such as the hepatoma cell lines HepaRG™ and Hep3B. Initially, HepaRG cells were discarded due to their specific media and supplement requirements. Unlike HepG2 cells, Hep3B cells do not form single cell colonies, which is necessary for selecting CRISPR modified cell clones. Thus, we selected the HepG2 cell line because of the easy handling of the cell culture, the expression of the *PMM2* gene, and the lack of chromosomic alterations of chromosome 16, where *PMM2* is located. Additionally, we emphasize the potential of these cancer cells to survive *PMM2* depletion, a gene that is essential for life [1,39,61,62], due to its tumoral nature. This characteristic is, however, a "double-edged sword": it allows us to study how these cells can survive the absence of PMM2 activity, but it can also distort the metabolic impairment due to the glycosylation deficiency [9]. This fact should be carefully considered in order to using our model to unravel pathophysiological events.

The obtained PMM2 KO HepG2 cells exhibited a complete absence of *PMM2* mRNA and PMM2 protein, reduced residual PMM activity, and altered glycosylation supported by the inability to fully glycosylate ICAM-1, LAMP1, and A1AT. PMM2 protein levels, PMM enzymatic activity, and the defect on glycosylation are recovered when the KO cells are transduced with the WT *PMM2* cDNA, corroborating the specificity of the pathological phenotype and indicating the potential use of this model to rescue the activity and function of PMM2 with candidate drugs.

We highlight that, although the HepG2-KO has no *PMM2* mRNA nor PMM2 protein, it retains some residual PMM activity. The ICAM-1, LAMP1 and A1AT glycosylation patterns are altered, however, the PNGaseF treatment of HepG2-KO cell extract suggests that the lack of PMM activity did not completely prevent the addition of glycans to the asparagine residues of these glycoproteins. We believe that there are likely other pathways that use the same substrates as PMM2 and could partially compensate for its absence in this cellular model. Further research in this area will help to clarify the source of this residual PMM activity. It is also unexpected that the HepG2-KO cells are able to proliferate normally, since we have reported a proliferation defect in some PMM2-CDG patient's fibroblasts [63]. In addition, it was recently described that *PMM2* depletion in a breast cancer cell line caused the inhibition of proliferation by reducing the mRNA and protein levels of estrogen receptor α [64]. It is a possibility that specific alterations in different metabolic pathways described in HepG2 cells could enable their survival and proliferation in the absence of PMM activity [65]. If so, these alterations could impede the study of some important aspects of the pathophysiology of PMM2-CDG related with proliferation, sugar metabolism and bioenergetics [8,9,66], limiting the scope of our HepG2 model.

Despite its constraints, this model offers an opportunity to study alternative pathways that compensate for *PMM2* deficiency through gene expression analysis [67] and to confirm and validate previous data obtained from RNA-seq studies with patients´ fibroblasts [63]. Additionally, these cells can be used to identify biomarkers for evaluating the therapeutic efficacy of new drugs *via* manifesting the potential recovery of the pathogenic phenotype. Since PMM2 is involved in the glycosylation of glycoconjugates, in this project, three glycoproteins (ICAM-1, LAMP1 and A1AT) were chosen as glycosylation biomarkers for the evaluation of clinical variants. The glycosylation pattern of these markers is remarkably altered in the HepG2-KO cells and in the HepG2-KO cells transduced with the empty GFP vector or with the FLAG LV-R123*, suggesting that these glycoproteins could be used as an endpoint to measure glycosylation alteration.

The first step in the variants´ assessment was the measurement of the PMM enzymatic activity in both lentiviral systems. This study allowed us also to compare both systems. The results obtained in this model corroborate and supplement the findings previously derived from the prokaryotic system and the structure-based analysis of pathogenic variants [31,35,37]. All the mutant proteins exhibit reduced activity between 6.4% and 42.5% for those expressed as GFP fusion proteins, and 8.3% and 21.6% for those carrying the FLAG tag. Generally, the enzymatic activity of the GFP mutants was higher than the enzymatic activity of the corresponding FLAG mutants, pointing out a possible stabilizing effect of the GFP. The potential stabilization of some mutants fused to GFP should be carefully considered since there are precedents of this stabilizing effect on recombinant mutant proteins fused to a glutathione S-transferase (GST) tag of 26 kDa [34]. The FLAG system provides a more physiological approach since FLAG is a 1-kDa-peptide, while GFP has a molecular weight of 27 kDa, the same as the PMM2 monomer [3]. After considering the advantages and limitations of each system, we have concluded that the best system for further studies aimed at demonstrating the effect of novel variants is the HepG2 system transduced with LV-FLAG.

Secondly, we evaluated the levels of PMM2, as well as the three glycoproteins, ICAM1, LAMP-1 and A1AT by western blotting. We observed that apart from the p.Arg123* mutant, there were no changes in ICAM1, and only some mutants showed a "smeared" LAMP1 pattern. The A1AT band pattern in the cell lines with the mutants closely resembled that of the WT HepG2 cells rather than the pattern observed in the KO cells or in the LV-WT recovered cells. We were unable to establish any correlation between the alterations of the three glycoproteins and the enzymatic activity levels of the selected clinical variants.

On the other hand, the HepG2-KO model of the p.Thr18Ser, p.Asp65Gly, and p.Thr237Lys variants of uncertain significance has allowed a deeper evaluation of their effect, which was not possible only with the prokaryotic expression system [31]. The p.Thr18Ser mutant exhibited protein stability similar to LV-WT and 60% enzymatic activity, confirming the non-pathogenic character of this variant. The p.Asp65Gly mutant, detected at lower levels than the LV-WT PMM2 protein, can be confirmed as a severe pathogenic variant with around 5% residual activity. The p.Thr237Lys mutant showed undetectable PMM2 protein and PMM enzymatic activity and displayed altered LAMP1 glycosylation, so it should also be considered a severe pathogenic variant. p.Thr237Lys and p.Asp65Gly pathogenic variants have been found in patients in combination with the severe p.Pro113Leu and p.Phe157Ser variants, respectively, suggesting a very severe phenotype.

Taken together, our results suggest that a slight increase in the PMM enzymatic activity has an essential impact on glycosylation, given that the glycosylation of the selected glycoproteins is rescued when the KO cells are transduced with some of the mutants included in this study, except for p.Pro113Leu, p.Arg162Trp and p.Thr237Met, and p.Thr237Lys. Retaining some residual enzymatic activity is enough to rescue the glycosylation process, at least *in vitro*. In line with this last statement, a recent study in PMM2-CDG patients´ fibroblasts also showed that the increase of PMM2 protein levels *via* AAV9-based *PMM2* gene replacement improves ICAM-1 and LAMP1 glycosylation [60]. Indeed, the possibility of rescuing PMM2-CDG phenotype through the increase of PMM2 concentration and/or activity has already been explored with therapeutic purposes [24,25,68–70]. However, it is still necessary to find more robust biomarkers to have a reliable readout when studying a new therapeutic strategy. ICAM1, LAMP-1 and A1AT act as good glycosylation markers when the glycosylation pathway is completely blocked, but are less reliable when the blockade is partial. Instead, we could evaluate the Halo3N reporter developed by Joseph N. Contessa's lab [71] as an alternative to assess the effect on N-glycosylation of the PMM2 studied variants, as well as the potential recovery after treatment. Additionally, glycoproteomics analysis could also be performed to reveal global changes in glycopeptides [72,73].

The results presented in this work indicate that the HepG2 model is an easy and quick high-throughput system to evaluate the pathogenic effect of clinical variants identified in PMM2-CDG cases and preventive

medicine by neonatal or carrier screening [28,29]. Moreover, this system could also be used to study other affected pathways identified in patients´ fibroblasts, such us the unfolded protein response due to endoplasmic reticulum stress [9], cell adhesion, and composition and organization of the extracellular matrix [63]. Its application could be extended to other CDGs with hepatic affectation. In fact, HepG2 cells have recently been used to demonstrate the importance of lipophagy in two novel CDGs associated with fatty liver disease, TMEM199-CDG and CCDC115-CDG [74]. In addition, it could be the initial step to evaluate the effectiveness of specific advanced therapies.

In summary, we have developed a high-performance diagnostic system for assessing the impact of variants on PMM activity and PMM2 stability. This platform for variant characterization could also be applied in biomarker identification and drug evaluation for PMM2-CDG or for other CDGs with liver involvement.

Funding

This work was funded by *Instituto de Salud Carlos* III (ISCIII), European Regional Development Fund [PI22/00699] to BP. The *CIBER de Enfermedades Raras* is an initiative from the ISCIII (Spain).

CRediT authorship contribution statement

Alicia Vilas: Writing – original draft, Methodology, Investigation, Formal analysis, Data curation. **Álvaro Briso-Montiano:** Methodology, Investigation, Data curation. **Cristina Segovia-Falquina:** Methodology, Investigation, Data curation. **Arturo Martín-Martínez:** Methodology, Investigation, Data curation. **Alejandro Soriano-Sexto:** Methodology, Investigation, Data curation. **Diana Gallego:** Methodology, Investigation, Data curation. **Vera Ruiz-Montés:** Methodology, Investigation. **Alejandra Gámez:** Writing – review & editing, Validation. **Belén Pérez:** Conceptualization, Funding acquisition, Supervision, Validation, Visualization, Project administration, Writing – review & editing.

Declaration of competing interest

The authors declare that they do not have any known personal or financial interests that could have affected the work that is described in this manuscript.

Data availability

Data will be made available on request.

Acknowledgments

We wholeheartedly thank the Spanish families affected by PMM2-CDG who actively participated in this research.

Appendix A. Supplementary data

Supplementary data to this article can be found online at https://doi.org/10.1016/j.ymgme.2024.108538.

References

[1] G. Matthijs, et al., Mutations in PMM2 that cause congenital disorders of glycosylation, type Ia (CDG-Ia), Hum. Mutat. 16 (5) (2000) 386–394, https://doi.org/10.1002/1098-1004(200011)16:5<386::AID-HUMU2>3.0.CO;2-Y.

[2] M.-A. Vals, S. Pajusalu, M. Kals, R. Mägi, Y.K. Õunap, The prevalence of PMM2-CDG in Estonia based on population carrier frequencies and diagnosed patients, JIMD Rep. 39 (2017) 13–17, https://doi.org/10.1007/8904_2017_41.

[3] G. Matthijs, et al., Mutations in PMM2, a phosphomannomutase gene on chromosome 16p13, in carbohydrate-deficient glycoprotein type I syndrome (Jaeken syndrome), Nat. Genet. 16, n.o 1 (1997) 88–92, https://doi.org/10.1038/ng0597-88.

[4] S. Grünewald, E. Schollen, E. Van Schaftingen, J. Jaeken, Y.G. Matthijs, High residual activity of PMM2 in Patients' fibroblasts: possible pitfall in the diagnosis of CDG-Ia (Phosphomannomutase deficiency), Am. J. Hum. Genet. 68 (2001) 347–354, https://doi.org/10.1086/318199.

[5] D. J. Lefeber, H. H. Freeze, R. Steet, T. Kinoshita, «Congenital disorders of glycosylation», en Essentials of Glycobiology, 4th ed., A. Varki, R. D. Cummings, J. D. Esko, P. Stanley, G. W. Hart, M. Aebi, D. Mohnen, T. Kinoshita, N. H. Packer, J. H. Prestegard, R. L. Schnaar, P. H. Seeberger, Eds., Cold Spring Harbor (NY): Cold Spring Harbor Laboratory Press, 2022. Accedido: 4 de enero de 2023. [En línea]. Disponible en: http://www.ncbi.nlm.nih.gov/books/NBK579928/.

[6] B. Cylwik, M. Naklicki, L. Chrostek, E. Gruszewska, Congenital disorders of glycosylation. Part I. Defects of protein N-glycosylation, Acta Biochim. Pol. 60 (2) (2013) 151–161.

[7] S. Radenkovic, et al., Tracer metabolomics reveals the role of aldose reductase in glycosylation, Cell Rep. Med. 4 (6) (2023), https://doi.org/10.1016/j.xcrm.2023.101056.

[8] A.N. Ligezka, et al., Interplay of impaired cellular bioenergetics and autophagy in PMM2-CDG, Genes 14 (8) (2023) 1585, https://doi.org/10.3390/genes14081585.

[9] L. Zdrazilova, et al., Metabolic adaptation of human skin fibroblasts to ER stress caused by glycosylation defect in PMM2-CDG, Mol. Genet. Metab. 139 (4) (2023) 107629, https://doi.org/10.1016/j.ymgme.2023.107629.

[10] N. Himmelreich, L.T. Kaufmann, H. Steinbeisser, C. Körner, C. Thiel, Lack of phosphomannomutase 2 affects Xenopus laevis morphogenesis and the non-canonical Wnt5a/Ror2 signalling, J. Inherit. Metab. Dis. 38 (6) (2015) 1137–1146, https://doi.org/10.1007/s10545-015-9874-0.

[11] S. Grunewald, The clinical spectrum of phosphomannomutase 2 deficiency (CDG-Ia), Biochim. Biophys. Acta 1792 (9) (2009) 827–834, https://doi.org/10.1016/j.bbadis.2009.01.003.

[12] R. Peanne, et al., Congenital disorders of glycosylation (CDG): quo vadis? Eur. J. Med. Genet. 61 (11) (2018) 643–663, https://doi.org/10.1016/j.ejmg.2017.10.012.

[13] S. Vuillaumier-Barrot, B. Isidor, T. Dupré, C. Le Bizec, A. David, N. Seta, Expanding the spectrum of PMM2-CDG phenotype, JIMD Rep. 5 (2011) 123–125, https://doi.org/10.1007/8904_2011_114.

[14] D. Coman, et al., Congenital disorder of glycosylation type 1a: three siblings with a mild neurological phenotype, J. Clin. Neurosci. 14 (7) (2007) 668–672, https://doi.org/10.1016/j.jocn.2006.04.008.

[15] S. Kjaergaard, M. Schwartz, F. Skovby, Congenital disorder of glycosylation type Ia (CDG-Ia): phenotypic spectrum of the R141H/F119L genotype, Arch. Dis. Child. 85 (3) (2001) 236–239, https://doi.org/10.1136/adc.85.3.236.

[16] P. de Lonlay, et al., A broad spectrum of clinical presentations in congenital disorders of glycosylation I: a series of 26 cases, J. Med. Genet. 38 (1) (2001) 14–19, https://doi.org/10.1136/jmg.38.1.14.

[17] F. Eyskens, C. Ceuterick, J.-J. Martin, G. Janssens, J. Jaeken, Carbohydrate-deficient glycoprotein syndrome with previously unreported features, Acta Paediatr. 83 (8) (1994) 892–896, https://doi.org/10.1111/j.1651-2227.1994.tb13166.x.

[18] B. Pérez-Dueñas, et al., Long-term evolution of eight Spanish patients with CDG type Ia: typical and atypical manifestations, Eur. J. Paediatr. Neurol. 13 (5) (2009) 444–451, https://doi.org/10.1016/j.ejpn.2008.09.002.

[19] R. Altassan, et al., International clinical guidelines for the management of phosphomannomutase 2-congenital disorders of glycosylation: diagnosis, treatment and follow up, J. Inherit. Metab. Dis. 42 (1) (2019) 5–28, https://doi.org/10.1002/jimd.12024.

[20] J. Jaeken, H.G. van Eijk, C. van der Heul, L. Corbeel, R. Eeckels, E. Eggermont, Sialic acid-deficient serum and cerebrospinal fluid transferrin in a newly recognized genetic syndrome, Clin. Chim. Acta 144 (2) (1984) 245–247, https://doi.org/10.1016/0009-8981(84)90059-7.

[21] V. Sharma, et al., Phosphomannose isomerase inhibitors improve N-glycosylation in selected phosphomannomutase-deficient fibroblasts, J. Biol. Chem. 286 (45) (2011) 39431–39438, https://doi.org/10.1074/jbc.M111.285502.

[22] S. Iyer, et al., Repurposing the aldose reductase inhibitor and diabetic neuropathy drug epalrestat for the congenital disorder of glycosylation PMM2-CDG, Dis. Model. Mech. 12 (11) (2019), https://doi.org/10.1242/dmm.040584.

[23] A.F. Martínez-Monseny, et al., AZATAX: acetazolamide safety and efficacy in cerebellar syndrome in PMM2 congenital disorder of glycosylation (PMM2-CDG), Ann. Neurol. 85 (5) (2019) 740–751, https://doi.org/10.1002/ana.25457.

[24] P. Yuste-Checa, et al., Pharmacological chaperoning: a potential treatment for PMM2-CDG, Hum. Mutat. 38 (2) (2017) 160–168, https://doi.org/10.1002/humu.23138.

[25] A. Vilas, et al., Proteostasis regulators as potential rescuers of PMM2 activity, Biochim. Biophys. Acta (BBA) - Mol. Basis Dis. 1866 (7) (2020) 165777, https://doi.org/10.1016/j.bbadis.2020.165777.

[26] C. Pérez-Cerdá, et al., A population-based study on congenital disorders of protein N- and combined with O-glycosylation experience in clinical and genetic diagnosis, J. Pediatr. 183 (2017) 170–177.e1, https://doi.org/10.1016/j.jpeds.2016.12.060.

[27] C.G. Asteggiano, et al., Ten years of screening for congenital disorders of glycosylation in Argentina: case studies and pitfalls, Pediatr. Res. 84 (6) (2018), https://doi.org/10.1038/s41390-018-0206-6.

[28] A.R. Gregg, et al., Screening for autosomal recessive and X-linked conditions during pregnancy and preconception: a practice resource of the American College of Medical Genetics and Genomics (ACMG), Genet. Med. 23 (10) (2021) 1793–1806, https://doi.org/10.1038/s41436-021-01203-z.

[29] A.D. Archibald, et al., The Australian reproductive genetic carrier screening project (Mackenzie's Mission): design and implementation, J. Pers. Med. 12 (11) (2022) 1781, https://doi.org/10.3390/jpm12111781.

[30] L. Hoffman-Andrews, The known unknown: the challenges of genetic variants of uncertain significance in clinical practice, J. Law Biosci. 4 (3) (2018) 648–657, https://doi.org/10.1093/jlb/lsx038.
[31] C. Segovia-Falquina, et al., A functional platform for the selection of pathogenic variants of PMM2 amenable to rescue via the use of pharmacological chaperones, Hum. Mutat. 43 (10) (2022) 1430–1442, https://doi.org/10.1002/humu.24431.
[32] S.S. Singh, Preclinical pharmacokinetics: an approach towards safer and efficacious drugs, Curr. Drug Metab. 7 (2) (2006) 165–182.
[33] A. Egesten, H. Herwald, «Modelers Modelling Models», J. Innate Immun., vol. 13, n.º 2, pp. 61–62, mar. 2021, doi: https://doi.org/10.1159/000515202.
[34] A.I. Vega, et al., Expression analysis revealing destabilizing mutations in phosphomannomutase 2 deficiency (PMM2-CDG): expression analysis of PMM2-CDG mutations, J. Inherit. Metab. Dis. 34 (4) (2011) 929–939, https://doi.org/10.1007/s10545-011-9328-2.
[35] P. Yuste-Checa, et al., The effects of PMM2-CDG-causing mutations on the folding, activity, and stability of the PMM2 protein, Hum. Mutat. 36 (9) (2015) 851–860, https://doi.org/10.1002/humu.22817.
[36] C.T. Thiesler, et al., Glycomic characterization of induced pluripotent stem cells derived from a patient suffering from Phosphomannomutase 2 congenital disorder of glycosylation (PMM2-CDG), Mol. Cell. Proteomics 15 (4) (2016) 1435–1452, https://doi.org/10.1074/mcp.M115.054122.
[37] A. Briso-Montiano, et al., Insight on molecular pathogenesis and pharmacochaperoning potential in phosphomannomutase 2 deficiency, provided by novel human phosphomannomutase 2 structures, J. Inherit. Metab. Dis. 45 (2) (2022) 318–333, https://doi.org/10.1002/jimd.12461.
[38] D. Quelhas, et al., Assessing the effects of PMM2 variants on protein stability, Mol. Genet. Metab. 134 (4) (2021) 344–352, https://doi.org/10.1016/j.ymgme.2021.11.002.
[39] C. Thiel, T. Lubke, G. Matthijs, K. von Figura, C. Korner, Targeted disruption of the mouse phosphomannomutase 2 gene causes early embryonic lethality, Mol. Cell. Biol. 265 (1) (2006) 5615–5620, https://doi.org/10.1128/MCB.02391-05.
[40] A. Schneider, et al., Successful prenatal mannose treatment for congenital disorder of glycosylation-Ia in mice, Nat. Med. 18 (1) (2011) 71–73, https://doi.org/10.1038/nm.2548.
[41] W.M. Parkinson, et al., Synaptic roles for phosphomannomutase type 2 in a new Drosophila congenital disorder of glycosylation disease model, Dis. Model. Mech. 9 (5) (2016) 513–527, https://doi.org/10.1242/dmm.022939.
[42] A. Cline, et al., A zebrafish model of PMM2-CDG reveals altered neurogenesis and a substrate-accumulation mechanism for N-linked glycosylation deficiency, Mol. Biol. Cell 23 (21) (2012) 4175–4187, https://doi.org/10.1091/mbc.E12-05-0411.
[43] K. Mukaigasa, et al., Nrf2 activation attenuates genetic endoplasmic reticulum stress induced by a mutation in the phosphomannomutase 2 gene in zebrafish, Proc. Natl. Acad. Sci. USA 115 (11) (2018) 2758–2763, https://doi.org/10.1073/pnas.1714056115.
[44] B. Chan, et al., A mouse model of a human congenital disorder of glycosylation caused by loss of PMM2, Hum. Mol. Genet. 25 (11) (2016) 2182–2193, https://doi.org/10.1093/hmg/ddw085.
[45] E. J. Klaver *et al.*, «Protease-dependent defects in N-cadherin processing drive PMM2-CDG pathogenesis», JCI Insight, 6, 24, e153474, doi: https://doi.org/10.1172/jci.insight.153474.
[46] P.-H.D. Edqvist, et al., Expression of human skin-specific genes defined by transcriptomics and antibody-based profiling, J. Histochem. Cytochem. 63 (2) (2015) 129–141, https://doi.org/10.1369/0022155414562646.
[47] L. Hayflick, The limited in vitro lifetime of human diploid cell strains, Exp. Cell Res. 37 (3) (1965) 614–636, https://doi.org/10.1016/0014-4827(65)90211-9.
[48] V.J. Cristofalo, R.J. Pignolo, Replicative senescence of human fibroblast-like cells in culture, Physiol. Rev. 73 (3) (1993) 617–638, https://doi.org/10.1152/physrev.1993.73.3.617.
[49] S. Akiyama, «[4] HeLa cell lines», en Methods in Enzymology, 151, Academic Press, 1987, 38–50. doi: https://doi.org/10.1016/S0076-6879(87)51007-2.
[50] M. T. Donato, R. Jover, y M. J. Gómez-Lechón, «Hepatic cell lines for drug hepatotoxicity testing: limitations and strategies to upgrade their metabolic competence by gene engineering», Curr. Drug Metab., 14, 9, 946–968.
[51] H. Xie, L. Hu, G. Li, SH-SY5Y human neuroblastoma cell line:in vitrocell model of dopaminergic neurons in Parkinson's disease, Chin. Med. J. 123 (8) (2010) 1086, https://doi.org/10.3760/cma.j.issn.0366-6999.2010.08.021.
[52] M. Irfan Maqsood, M.M. Matin, A.R. Bahrami, M.M. Ghasroldasht, Immortality of cell lines: challenges and advantages of establishment, Cell Biol. Int. 37 (10) (2013) 1038–1045, https://doi.org/10.1002/cbin.10137.
[53] M.M. Shipley, C.A. Mangold, M.L. Szpara, Differentiation of the SH-SY5Y human neuroblastoma cell line, J. Vis. Exp. 108 (2016) 53193, https://doi.org/10.3791/53193.
[54] S.W. Cho, S. Kim, J.M. Kim, J.S. Kim, Targeted genome engineering in human cells with the Cas9 RNA-guided endonuclease, Nat. Biotechnol. 31 (3) (2013) 3, https://doi.org/10.1038/nbt.2507.
[55] F.A. Ran, P.D. Hsu, J. Wright, V. Agarwala, D.A. Scott, F. Zhang, Genome engineering using the CRISPR-Cas9 system, Nat. Protoc. 8 (11) (2013) 2281–2308, https://doi.org/10.1038/nprot.2013.143.
[56] F. Sanger, S. Nicklen, A.R. Coulson, DNA sequencing with chain-terminating inhibitors, Proc. Natl. Acad. Sci. USA 74 (12) (1977) 5463–5467.
[57] E. Van Schaftingen, J. Jaeken, Phosphomannomutase deficiency is a cause of carbohydrate-deficient glycoprotein syndrome type I, FEBS Lett. 377 (3) (1995) 318–320, https://doi.org/10.1016/0014-5793(95)01357-1.
[58] T.J. de Koning, et al., A novel disorder of N-glycosylation due to phosphomannose isomerase deficiency, Biochem. Biophys. Res. Commun. 245 (1) (1998) 38–42, https://doi.org/10.1006/bbrc.1998.8385.
[59] E. Richard, L.R. Desviat, M. Ugarte, B. Pérez, Oxidative stress and apoptosis in homocystinuria patients with genetic remethylation defects, J. Cell. Biochem. 114 (1) (2013) 183–191, https://doi.org/10.1002/jcb.24316.
[60] M. Zhong, B. Balakrishnan, A.J. Guo, K. Lai, AAV9-based PMM2 gene replacement augments PMM2 expression and improves glycosylation in primary fibroblasts of patients with phosphomannomutase 2 deficiency (PMM2-CDG), Mol. Genet. Metab. Rep. 38 (2023) 101035, https://doi.org/10.1016/j.ymgmr.2023.101035.
[61] G. Matthijs, E. Schollen, E. Van Schaftingen, J.J. Cassiman, J. Jaeken, Lack of homozygotes for the most frequent disease allele in carbohydrate-deficient glycoprotein syndrome type 1A, Am. J. Hum. Genet. 62 (3) (1998) 542–550.
[62] E. Schollen, S. Kjaergaard, E. Legius, M. Schwartz, G. Matthijs, Lack of hardy-Weinberg equilibrium for the most prevalent PMM2 mutation in CDG-Ia (congenital disorders of glycosylation type Ia), Eur. J. Hum. Genet. 8 (5) (2000) 5, https://doi.org/10.1038/sj.ejhg.5200470.
[63] D. Gallego, et al., Transcriptomic analysis identifies dysregulated pathways and therapeutic targets in PMM2-CDG, Biochim. Biophys. Acta Mol. basis Dis. 1870 (5) (2024) 167163, https://doi.org/10.1016/j.bbadis.2024.167163.
[64] M. Cipolletti, F. Acconcia, PMM2 controls ERα levels and cell proliferation in ESR1 Y537S variant expressing breast cancer cells, Mol. Cell. Endocrinol. 584 (2024) 112160, https://doi.org/10.1016/j.mce.2024.112160.
[65] O.I. Kiseleva, et al., Exploring dynamic metabolome of the HepG2 cell line: rise and fall, Cells 11 (22) (2022) 3548, https://doi.org/10.3390/cells11223548.
[66] N. Himmelreich, et al., Complex metabolic disharmony in PMM2-CDG paves the way to new therapeutic approaches, Mol. Genet. Metab. 139 (3) (2023) 107610, https://doi.org/10.1016/j.ymgme.2023.107610.
[67] F.M. Jabato, et al., Gene expression analysis method integration and co-expression module detection applied to rare glucide metabolism disorders using ExpHunterSuite, Sci. Rep. 11 (1) (2021) 15062, https://doi.org/10.1038/s41598-021-94343-w.
[68] D. Thirumal Kumar, N. Jain, S. Udhaya Kumar, C. George Priya Doss, H. Zayed, Identification of potential inhibitors against pathogenic missense mutations of PMM2 using a structure-based virtual screening approach, J. Biomol. Struct. Dyn. (2020) 1–17, https://doi.org/10.1080/07391102.2019.1708797.
[69] M. Monticelli, L. Liguori, M. Allocca, G. Andreotti, M.V. Cubellis, β-Glucose-1,6-bisphosphate stabilizes pathological Phophomannomutase2 mutants in vitro and represents a Lead compound to develop pharmacological chaperones for the Most common disorder of glycosylation, PMM2-CDG, Int. J. Mol. Sci. 20 (17) (2019) 17, https://doi.org/10.3390/ijms20174164.
[70] J.P. Lao, N. DiPrimio, M. Prangley, F.S. Sam, J.D. Mast, E.O. Perlstein, Yeast models of phosphomannomutase 2 deficiency, a congenital disorder of glycosylation, G3 (2018) g3.200934, https://doi.org/10.1534/g3.118.200934.
[71] N. Rinis, et al., Editing N-glycan site occupancy with small-molecule oligosaccharyltransferase inhibitors, Cell Chem. Biol. 25 (10) (2018) 1231–1241.e4, https://doi.org/10.1016/j.chembiol.2018.07.005.
[72] R. Budhraja, et al., Liposome-encapsulated mannose-1-phosphate therapy improves global N-glycosylation in different congenital disorders of glycosylation, Mol. Genet. Metab. 142 (2024) 108487, https://doi.org/10.1016/j.ymgme.2024.108487.
[73] H.J.C.T. Wessels, et al., Plasma glycoproteomics delivers high-specificity disease biomarkers by detecting site-specific glycosylation abnormalities, J. Adv. Res. 61 (2024) 179–192, https://doi.org/10.1016/j.jare.2023.09.002.
[74] L.E. Larsen, et al., Defective lipid droplet-lysosome interaction causes fatty liver disease as evidenced by human mutations in TMEM199 and CCDC115, Cell. Mol. Gastroenterol. Hepatol. 13 (2022) 583–597, https://doi.org/10.1016/j.jcmgh.2021.09.013.